applied sciences

MDPI

Supplementary Materials

A comparison of palladium sorption using polyethylenimine impregnated alginate-based and carrageenan-based algal beads

Shengye Wang [1*], Thierry Vincent [1], Catherine Faur [2] and Eric Guibal [1*]

[1] C2MA, IMT Mines Ales, Univ Montpellier, Ales, France; Shengye.Wang@mines-ales.fr; Thierry.Vincent@mines-ales.fr

[2] IEM, Institut Européen des membranes, Univ Montpellier, CNRS, ENSCM, Montpellier, France; Catherine.Faur@umontpellier.fr

* Correspondence: Eric.Guibal@mines-ales.fr; Tel.: +33-046-678-2734

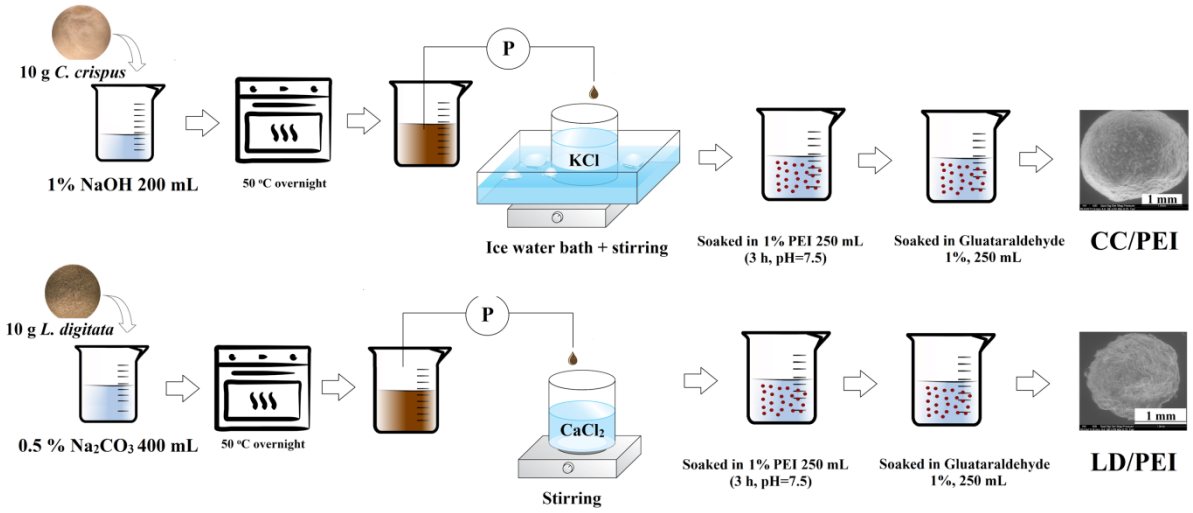

Figure S1. The preparation process of LD/PEI and CC/PEI beads.

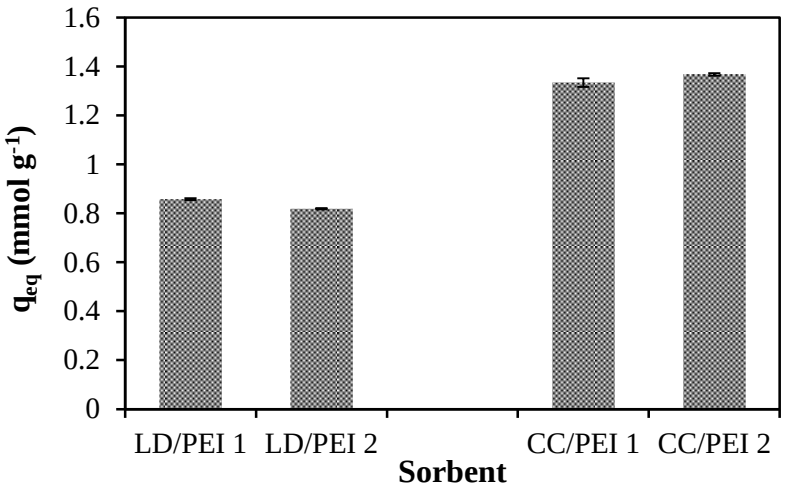

Figure S2. The sorption capacity of the beads prepared at two different times (Dose: 0.5 g L^{-1}; pH: 1-adjusted by H_2SO_4 or NaOH; Contact time: 72 h; T: 20 °C).

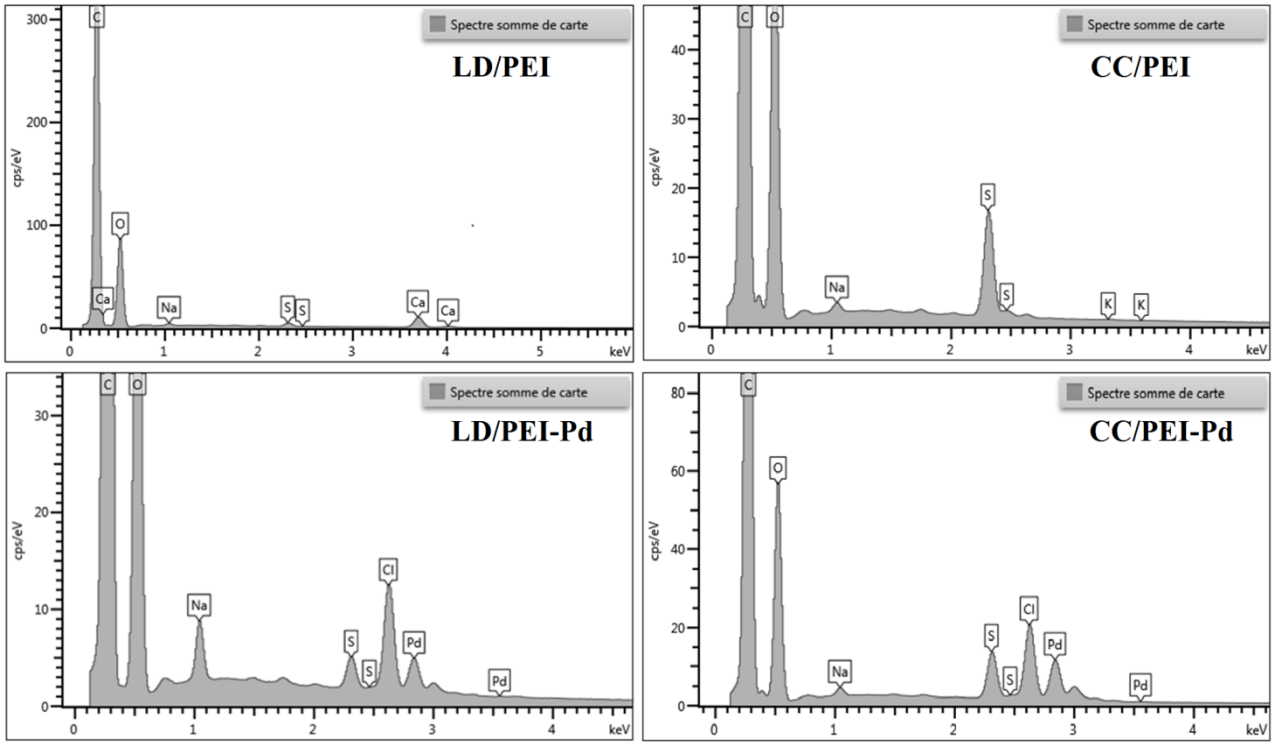

Figure S3. EDX analysis of LD/PEI and CC/PEI beads before and after Pd(II) sorption.

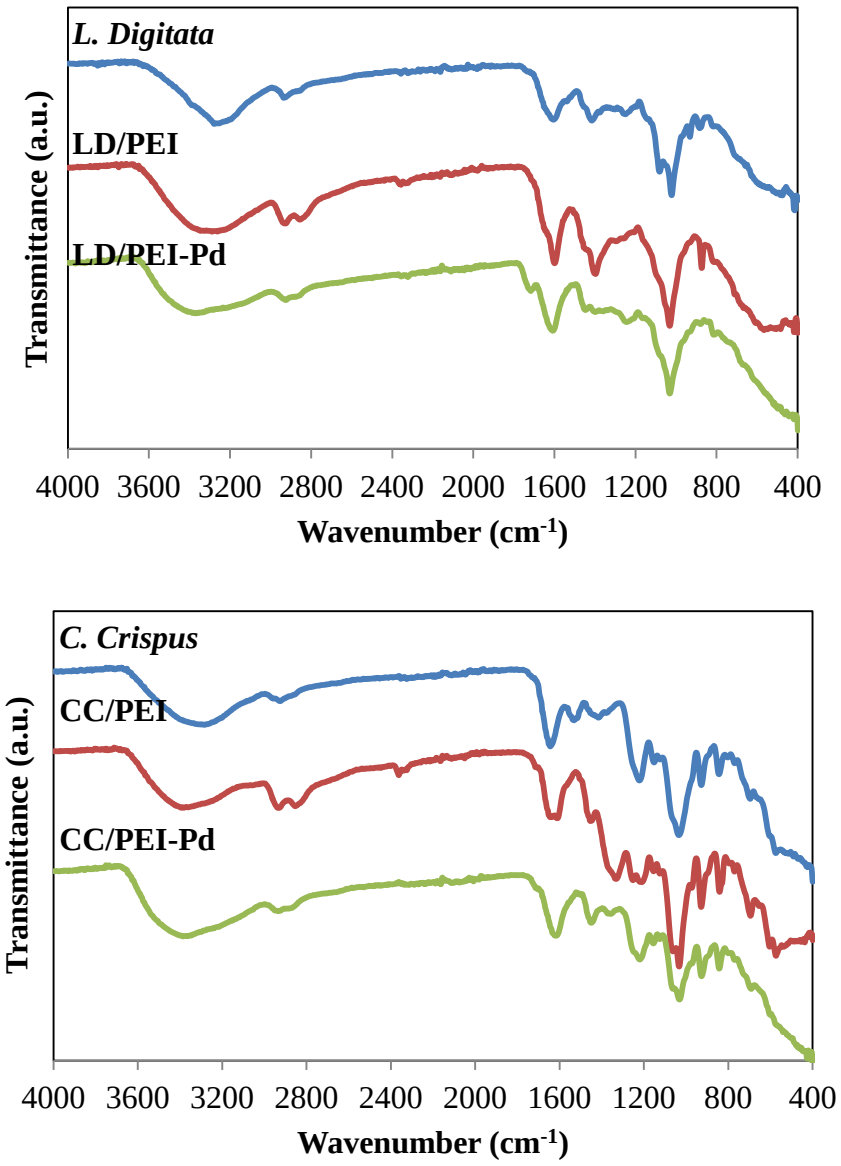

Figure S4. FTIR spectra of the raw biomass (*L. digitata* and *C. crispus*), beads (LD/PEI and CC/PEI) and the beads after loading with Pd(II).

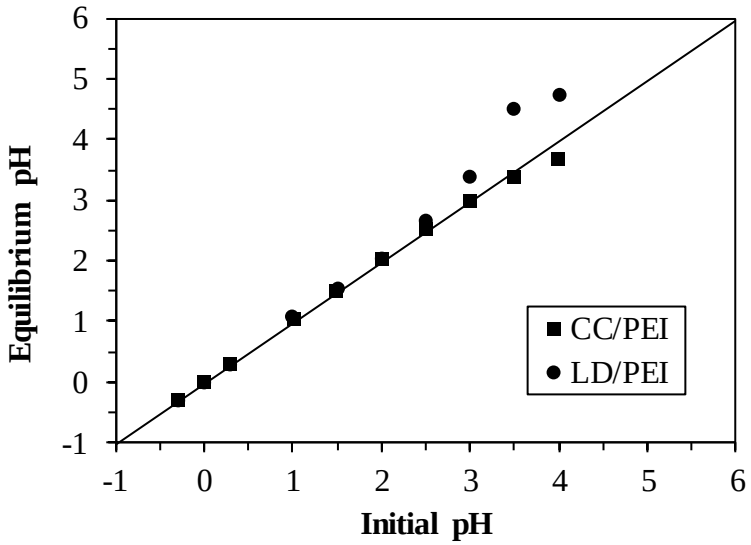

Figure S5. pH change after sorption process.

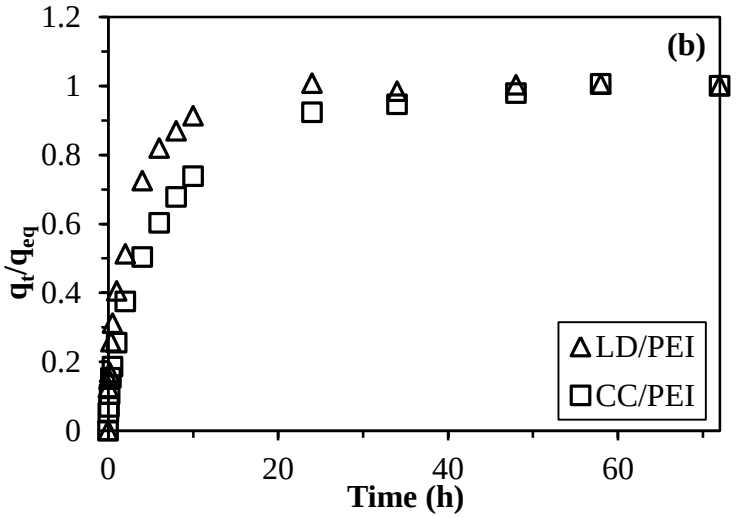

Figure S6. Plots of q_t/q_{eq} as a function of the time for Pd(II) sorption onto LD/PEI and CC/PEI beads.

Table S1. Experimental frequencies of the bands observed for the raw biomass (*L. digitata* and *C. crispus*), beads (LD/PEI and CC/PEI) and the beads after loading with Pd(II). Unit: cm^{-1}.

Vibration	**In reference**	***L. Digitata***			***C. Crispus***			**Ref.**
		Raw	**LD/PEI**	**LD/PEI-Pd**	**Raw**	**CC/PEI**	**CC/PEI-Pd**	
overlapping of –OH and N–H	3500-3000	3278	3289	3370	3283	3382	3386	[1,2]
C–H stretching	2928	2935	2926	2930	2924	2931	2934	[3]
C–H vibration	2856		2856	2853		2854	2855	[4]
Carboxylic acid C=O stretching (weakly hydrogen bonded)	1711			1716				[5]
C=C stretching	1644				1644			[6]
C=N vibration	1599		1599	1608		1610	1621	[2]
COO− asymmetric stretching	1605	1605						[7]
N–H bending	1531				1531			[8]
COO− symmetric stretching	1397, 1429	1416	1397		1416	1453	1449	[9,10]
C=O vibration	1350					1331	1358	[11]
S–O stretching	1154, 1221				1152, 1221	1154, 1210	1155, 1219	[12,13]
C–O stretching	1260	1250		1244				[14]
Si–O stretching	1081	1081						[15]
C–O–C antisym. stretching	1152, 1025	1022	1031	1031	1152, 1034	1154, 1032	1155, 1031	[16,17]
Al–OH vibration	932	932			927	928	926	[18]
C–Cl stretching	883	883	873		844	840	842	[19]
CH bending	696				696	694		[20]

Table S2: Pd(II) sorption properties of a series of sorbents.

Sorbent	pH	q_m (mmol g^{-1})	Ref.
R. lanuginosum biomass	5	0.35	[21]
Alginate beads	2.5	0.38	[22]
Algal beads	2.5	0.47	[22]
Montmorillonite modified alginate beads	4	0.93	[23]
Laponite modified alginate beads	4	1.38	[23]
Thiacalix[6]arene derivative impregnated XAD-7 resin	0.1 M HCl	0.18	[24]
Cyphos IL-101 impregnated XAD-7 resin	0.5 M HCl	0.67	[25]
p-Sulfonatothiacalix[6]arene-impregnated XAD-7 resin	4	1.29	[26]
p-Sulfonatothiacalix[6]arene-impregnated IRA-411 resin	4	2.73	[26]
p-Sulfonatothiacalix[6]arene-impregnated IRA-400 resin	4	2.86	[26]
LD/PEI	1	0.85	This study
CC/PEI	1	1.34	This study

Table S3. Palladium and anion species when 15 mM SO_4^{2-} (i.e., 5 mM $Fe_2(SO_4)_3$, 15 mM $CuSO_4$, or 5 mM $Al_2(SO4)_3$) were added.

Ions	Species name	% of total concentration		
		$Fe_2(SO_4)_3$	$Al_2(SO4)_3$	$CuSO_4$
Palladium	$PdCl_4^{2-}$	96.60	96.65	96.64
	$PdCl_3^-$	3.25	3.21	3.21
	$PdCl_2$ (aq)	0.15	0.14	0.14
Chloride	Cl^-	95.68	96.44	95.76
	metal complexes (anions)	3.45 - $PdCl_4^{2-}$ 0.09 - $PdCl_3^-$	3.45 - $PdCl_4^{2-}$ 0.09 - $PdCl_3^-$	3.45 - $PdCl_4^{2-}$ 0.09 - $PdCl_3^-$
	metal complexes (cations)	0.78 - $FeCl_2^+$	0.02 - $AlCl_2^+$	0.71 - $CuCl^+$
Sulfate	SO_4^{2-}	16.64	16.86	19.59
	HSO_4^-	67.07	67.23	74.60
	metal complexes (anions)	1.13 - $Fe(SO_4)_2^-$	3.71 - $Al(SO_4)_2^-$	5.18 - $CuSO_4$ (aq)
	metal complexes (cations)	15.16 - $FeSO_4^+$	12.19 - $AlSO_4^+$	0.62 - $CuHSO_4^-$

Note: the speciation was calculated by Visual MINTEQ (version 3.0).

References

1. Schiewer, S.; Balaria, A. Biosorption of Pb^{2+} by original and protonated citrus peels: equilibrium, kinetics, and mechanism. *Chem. Eng. J.* **2009**, *146*, 211-219.
2. Yu, Z.; Chuang, S.S. The effect of Pt on the photocatalytic degradation pathway of methylene blue over TiO_2 under ambient conditions. *Appl. Catal. B-Environ.* **2008**, *83*, 277-285.
3. Naebe, M.; Wang, J.; Amini, A.; Khayyam, H.; Hameed, N.; Li, L.H.; Chen, Y.; Fox, B. Mechanical property and structure of covalent functionalised graphene/epoxy nanocomposites. *Sci. Rep.* **2014**, *4*, 4375.

4. Azemard, C.; Vieillescazes, C.; Ménager, M. Effect of photodegradation on the identification of natural varnishes by FT-IR spectroscopy. *Microchem. J.* **2014**, *112*, 137-149.
5. Xiaohong, G.; Yang, C.Q. FTIR spectroscopy study of the formation of cyclic anhydride intermediates of polycarboxylic acids catalyzed by sodium hypophosphite. *Text. Res. J.* **2000**, *70*, 64-70.
6. Chung, C.-M.; Lee, S.-J.; Kim, J.-G.; Jang, D.-O. Organic–inorganic polymer hybrids based on unsaturated polyester. *J. Non-cryst. Solids* **2002**, *311*, 195-198.
7. Luo, J.; Wang, L.; Mott, D.; Njoki, P.N.; Kariuki, N.; Zhong, C.-J.; He, T. Ternary alloy nanoparticles with controllable sizes and composition and electrocatalytic activity. *J. Mater. Chem.* **2006**, *16*, 1665-1673.
8. Rosu, D.; Rosu, L.; Cascaval, C.N. IR-change and yellowing of polyurethane as a result of UV irradiation. *Polym. Degrad. Stabil.* **2009**, *94*, 591-596.
9. Hofmann, M.P.; Young, A.M.; Gbureck, U.; Nazhat, S.N.; Barralet, J.E. FTIR-monitoring of a fast setting brushite bone cement: effect of intermediate phases. *J. Mater. Chem.* **2006**, *16*, 3199-3206.
10. Theras, J.E.M.; Kalaivani, D.; Jayaraman, D.; Joseph, V. Growth and spectroscopic, thermodynamic and nonlinear optical studies of L-threonine phthalate crystal. *J. Cryst. Growth* **2015**, *427*, 29-35.
11. Sengupta, P.; Ghosh, S.; Mak, T.C. A new route for the synthesis of bis (pyridine dicarboxylato) bis (triphenylphosphine) complexes of ruthenium (II) and X-ray structural characterisation of the biologically active *trans*-[Ru (PPh 3) 2 (L 1 H) 2](L 1 H 2= pyridine 2, 3-dicarboxylic acid). *Polyhedron* **2001**, *20*, 975-980.
12. Tarulli, S.; Quinzani, O.; Piro, O.E.; Castellano, E.E.; Baran, E. Structural and spectroscopic characterization of bis (thiosaccharinato) bis (benzimidazole) cadmium (II). *J. Mol. Struct.* **2006**, *797*, 56-60.
13. Qiao, J.; Hamaya, T.; Okada, T. New highly proton-conducting membrane poly (vinylpyrrolidone)(PVP) modified poly (vinyl alcohol)/2-acrylamido-2-methyl-1-propanesulfonic acid (PVA–PAMPS) for low temperature direct methanol fuel cells (DMFCs). *Polymer* **2005**, *46*, 10809-10816.
14. Pavasant, P.; Apiratikul, R.; Sungkhum, V.; Suthiparinyanont, P.; Wattanachira, S.; Marhaba, T.F. Biosorption of Cu^{2+}, Cd^{2+}, Pb^{2+}, and Zn^{2+} using dried marine green macroalga *Caulerpa lentillifera*. *Bioresour. Technol.* **2006**, *97*, 2321-2329.
15. Ismail, H.; Shaari, S. Curing characteristics, tensile properties and morphology of palm ash/halloysite nanotubes/ethylene-propylene-diene monomer (EPDM) hybrid composites. *Polym. Test.* **2010**, *29*, 872-878.
16. Wang, X.; Li, D.; Wang, W.; Feng, Q.; Cui, F.; Xu, Y.; Song, X.; van der Werf, M. Crosslinked collagen/chitosan matrix for artificial livers. *Biomaterials* **2003**, *24*, 3213-3220.
17. Lawrie, G.; Keen, I.; Drew, B.; Chandler-Temple, A.; Rintoul, L.; Fredericks, P.; Grøndahl, L. Interactions between alginate and chitosan biopolymers characterized using FTIR and XPS. *Biomacromolecules* **2007**, *8*, 2533-2541.
18. Pasbakhsh, P.; Ismail, H.; Fauzi, M.A.; Bakar, A.A. Influence of maleic anhydride grafted ethylene propylene diene monomer (MAH-g-EPDM) on the properties of EPDM nanocomposites reinforced by halloysite nanotubes. *Polym. Test.* **2009**, *28*, 548-559.
19. Rajendran, S.; Uma, T. Lithium ion conduction in PVC–$LiBF_4$ electrolytes gelled with PMMA. *J. Power Sources* **2000**, *88*, 282-285.
20. Ríos-Gómez, J.; Lucena, R.; Cárdenas, S. Paper supported polystyrene membranes for thin film microextraction. *Microchem. J.* **2017**, *133*, 90-95.
21. Sari, A.; Mendil, D.; Tuzen, M.; Soylak, M. Biosorption of palladium (II) from aqueous solution by moss (*Racomitrium lanuginosum*) biomass: Equilibrium, kinetic and thermodynamic studies. *J. Hazard. Mater.* **2009**, *162*, 874-879.
22. Wang, S.; Vincent, T.; Roux, J.-C.; Faur, C.; Guibal, E. Pd (II) and Pt (IV) sorption using alginate and algal-based beads. *Chem. Eng. J.* **2017**, *313*, 567-579.

23. Cataldo, S.; Muratore, N.; Orecchio, S.; Pettignano, A. Enhancement of adsorption ability of calcium alginate gel beads towards Pd (II) ion. A kinetic and equilibrium study on hybrid Laponite and Montmorillonite–alginate gel beads. *Applied Clay Science* **2015**, *118*, 162-170.
24. Kimuro, T.; Gandhi, M.R.; Kunda, U.M.R.; Hamada, F.; Yamada, M. Palladium (II) sorption of a diethylphosphate-modified thiacalix [6] arene immobilized on amberlite resin. *Hydrometallurgy* **2017**.
25. Navarro, R.; Saucedo, I.; Gonzalez, C.; Guibal, E. Amberlite XAD-7 impregnated with Cyphos IL-101 (tetraalkylphosphonium ionic liquid) for Pd (II) recovery from HCl solutions. *Chem. Eng. J.* **2012**, *185*, 226-235.
26. Gandhi, M.R.; Yamada, M.; Kondo, Y.; Shibayama, A.; Hamada, F. *p*-Sulfonatothiacalix [6] arene-impregnated resins for the sorption of platinum group metals and effective separation of palladium from automotive catalyst residue. *Journal of Industrial and Engineering Chemistry* **2015**, *30*, 20-28.